

LNF-09/07 (IR)
June 25, 2009

**DYNAMICS OF BOUND STATE POPULATIONS FOR CHANNELED
ELECTRONS/POSITRONS**

A. Babaev^{1,2}, and S.B. Dabagov^{2,3}

¹Tomsk Polytechnic University, 634050 Tomsk, Russia

²INFN Laboratori Nazionali di Frascati, 00044 Frascati, Italy

³RAS PN Lebedev Physical Institute, 119991 Moscow, Russia

Abstract

When electrons or positrons are planar channeled through a crystal, the spectrum of bound energy states forms and one can observe so-called channeling radiation. The intensity of channeling radiation depends on populations of bound energy levels. These populations change during projectiles motion through a crystal that, in turn, influences the CR intensity. In this manuscript we present theoretical model and computer codes to investigate the bound energy spectra of planar-channeled electrons and positrons and to obtain the initial populations of bound states. Solving the kinetic equations and using some approximations we explore the dynamics of bound state populations. In the future taking into account the dechanneling processes more realistic picture of evolution of bound state populations will be giving.

PACS.: 61.85.+p

1 INTRODUCTION

When the charged particles moves in a crystal under small angles to the crystal planes or axes, the channeling motion may take place [1]. As known, interaction of light particles with a crystal potential under the channeling conditions forms the spectrum of bound energy states for projectiles [2]. The transitions between these energy levels at channeling result in channeling radiation (CR) [3]. The intensities of CR lines depend on populations of energy levels at the time of radiation.

Hence, to estimate the line intensity, one should know the dynamic of populations for bound states. The behaviors of populations are described by “the kinetic equations” [4]. In this work we present the solutions, describing the behavior of bound state populations under projectile planar channeling. We are considering the range of relatively small energies (less than 120 MeV), when the quantum-mechanical treatment is applicable to the particle dynamics (the number of sub-barrier levels is about 10-20).

2 BOUND ENERGY STATES AND WAVE FUNCTIONS

2.1 Crystal potential

As known the crystal potential forms as a sum of separate atomic potentials, and when a particle moves along a crystal plane under small glancing angle, the potential can be replaced by the averaged planar potential – “continuous planar potential” [2,3]. It is noteable that the potential averaging can be analytically performed keeping rather good agreement with experimentally observed data.

Let us consider a particle moving under planar channeling. We are directing the OX axis transverse to the crystal plane and the orthogonal OY and OZ axes parallel to the plane; the origin of OX axis is in the center of a channel (see Fig. 1). In this case the planar crystal potential may be represented by Fourier expansion:

$$U_{\text{pl}}(x, y, z) = \sum_{k_y, k_z} U_{k_y, k_z, \text{pl}}(x) \exp[i(k_y y + k_z z)]. \quad (1)$$

where k_y and k_z are the reciprocal lattice vectors of the plane:

$$k_y = \frac{2n_y \pi}{a_y}, \quad k_z = \frac{2n_z \pi}{a_z}, \quad (2)$$

with the integer numbers n_y and n_z , a_y and a_z are the distances between atoms in a plane. The main harmonic in expansion (1) with $n_y=n_z=0$ corresponds to the continuous planar potential $U_{0, \text{pl}}(x)$. Successfully, the functions $U_{k_y, k_z}(x)$ are the side harmonics amplitudes, which are decreasing at the numbers n_y and n_z increase.

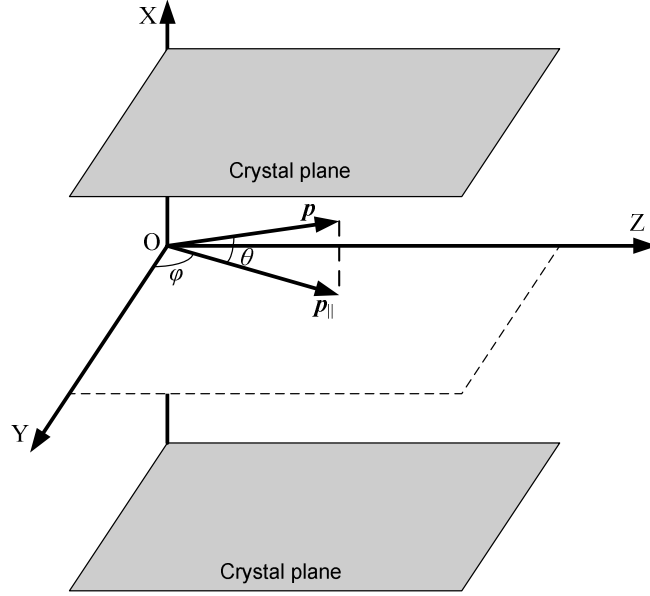


Fig.1. Scheme of the coordinate frame.

In this work we use the Moliere approximation for screened atomic potential, which, after averaging over all atoms in a plane and, successfully, over thermal atomic vibrations, can be reduced to next expressions for both continuous potential and side harmonics in expansion (2) [4]:

$$U_{0,pl}(\tilde{x}) = \frac{\pi \cdot Z_{cr} Z \alpha \hbar c a_{TF}}{a_y a_z} \cdot \sum_{i=1}^3 \exp\left(\frac{\beta_i^2 u^2}{2a_{TF}^2}\right) \cdot \left(\frac{\alpha_i}{\beta_i} \left(\exp\left(\beta_i \frac{|\tilde{x}|}{a_{TF}}\right) \operatorname{erfc}\left(\beta_i \frac{u}{\sqrt{2}a_{TF}} + \frac{|\tilde{x}|}{\sqrt{2}u}\right) + \exp\left(-\beta_i \frac{|\tilde{x}|}{a_{TF}}\right) \operatorname{erfc}\left(\beta_i \frac{u}{\sqrt{2}a_{TF}} - \frac{|\tilde{x}|}{\sqrt{2}u}\right) \right) \right) \quad (3)$$

$$U_{k_y, k_z, pl}(\tilde{x}) = \frac{\pi \cdot Z_{cr} Z \alpha \hbar c a_{TF}}{a_y a_z} \cdot \sum_{i=1}^3 \exp\left(\frac{\beta_{i, k_y, k_z}^2 u^2}{2a_{TF}^2}\right) \cdot \left(\frac{\alpha_i}{\beta_{i, k_y, k_z}} \left(\exp\left(\beta_{i, k_y, k_z} \frac{|\tilde{x}|}{a_{TF}}\right) \operatorname{erfc}\left(\beta_{i, k_y, k_z} \frac{u}{\sqrt{2}a_{TF}} + \frac{|\tilde{x}|}{\sqrt{2}u}\right) + \exp\left(-\beta_{i, k_y, k_z} \frac{|\tilde{x}|}{a_{TF}}\right) \operatorname{erfc}\left(\beta_{i, k_y, k_z} \frac{u}{\sqrt{2}a_{TF}} - \frac{|\tilde{x}|}{\sqrt{2}u}\right) \right) \right) \quad (4)$$

In these expressions \tilde{x} is the distance to the plane; the dimension of the potential is given in “energy” units. Here, Z_{cr} is the number of a lattice atom, Z equals 1 for positrons and -1 for electrons, \hbar is the Planck constant, α is the fine structure constant, c is the speed of light. The screening radius is expressed in the following approximation

$$a_{\text{TF}} = 0.88534 Z_{\text{cr}}^{-1/3} a_{\text{b}},$$

a_{b} is the Bohr radius. Parameters of Moliere potential are $\alpha_1=0.1$, $\alpha_2=0.55$, $\alpha_3=0.35$, $\beta_1=6.0$, $\beta_2=1.2$, $\beta_3=0.3$, $\beta_{i,k_y,k_z} = \sqrt{\beta_i^2 + a_{\text{TF}}^2 (k_y^2 + k_z^2)}$.

The expressions (3) and (4) are written for the planes when the cell of a plane consists of one atom. If the cell of a plane consists of two atoms and the vector (ρ_y, ρ_z) in the plane defines the displacement of these atoms, the expression (3) should be multiplied by the factor 2 and the expression (4) - by the factor $f_{\text{b}} = 1 + \exp(-i(k_y \rho_y + k_z \rho_z))$.

For simplicity we describe the crystal potential by a sum of potentials of two neighbor planes forming a channel for particle propagation. In this case the continuous potential of a crystal is evaluated by

$$U_0(x) = U_{0,\text{pl}}(d+x) + U_{0,\text{pl}}(d-x), \quad (5)$$

and the non-zero harmonic of periodic potential – by

$$U_{k_y,k_z}(x) = U_{k_y,k_z,\text{pl}}(x+d) + U_{k_y,k_z,\text{pl}}(d-x) \exp(-i(k_y y_{\text{pl}} + k_z z_{\text{pl}})), \quad (6)$$

the vector $(a_x, y_{\text{pl}}, z_{\text{pl}})$ defines the relative atoms disposition for two neighboring parallel planes, a_x is the distance between planes, $d=a_x/2$.

2.2 Bound energy spectrum

The total energy E of a channeled particle can be presented as a sum of longitudinal energy E_{\parallel} and transverse energy ε . On the first approximation, one can consider, that particle moves in a channel under influence of continuous potential only. The transverse energy has discrete values and is defined by Schrodinger-type equation [2]:

$$\left(-\frac{1}{2E_{\parallel}} \frac{d^2}{dx^2} + U_0(x) \right) \psi(x) = \varepsilon \psi(x). \quad (7)$$

The longitudinal energy is $E_{\parallel} = \sqrt{(m_0 c^2)^2 + (p_{\parallel} c)^2} - m_0 c^2$, $p_{\parallel} = p \cos \theta$ is longitudinal momentum, $p = \sqrt{\gamma^2 - 1} \cdot m_0 c$ is the full momentum of particle, $\gamma = \frac{E_{\text{kin}}}{m_0 c^2} + 1$, E_{kin} is the total kinetic energy of particle, θ is the angle between momentum of particle and crystal planes (see Fig. 1), $m_0 c^2$ is the rest energy of particle (electron or positron).

Due to the transverse periodicity of continuous potential (4), the wave functions and continuous potential can be presented by Fourier expansions [2]:

$$U_0(x) = \sum_m U_{0,m} \exp(img_0x), \quad (7)$$

$$\psi(x) = \sum_n C_n \exp(i(\kappa - ng_0)x). \quad (8)$$

In Eqs.(7) and (8) $g_0 = 2\pi/a_x$ is the reciprocal lattice vector, which is transverse to the planes, κ is the quasimomentum defined as:

$$\kappa = \frac{p_\perp}{\hbar} - Ng_0.$$

The integer number N is such that $-\frac{\pi}{a_x} < \kappa < \frac{\pi}{a_x}$, $p_\perp = p \sin \theta$ is the initial transverse momentum of channeled particle. In Eq. (7) $U_{0,m}$ are the Furrier components of continuous potential,

$$U_{0,m} = \int_{-d}^d U_0(x) \cos(mg_0x) dx,$$

as seen in this expression $U_0(x)$ is the even function; the coefficients C_n in Eq. (8) will be defined later. The presented expansions are cut off on the number N_{\max} when the Fourier components $U_{0,m}$ become rather small.

The use of Eqs.(7) and (8) in Schrodinger equation results in the following matrix equation:

$$\mathbf{M}\mathbf{C} = \varepsilon \cdot \mathbf{C}. \quad (9)$$

The symmetric matrix \mathbf{M} consists of the terms $M_{ii} = \frac{\hbar^2 c^2 (\kappa - ig_0)^2}{2E_{\parallel}} + U_{0,0}$ and

$M_{ij} = U_{0,(j-i)-2N_{\max}}$, $j \neq i$, $i, j = [-N_{\max}; N_{\max}]$; \mathbf{C} is the matrix with coefficients C_n , $n = [-N_{\max}; N_{\max}]$. The dimension of matrix \mathbf{M} is determined by $(2N_{\max}+1)$. Hence, one can obtain $(2N_{\max}+1)$ eigenvalues ε_i from Eq.(9) that defines the bound energy levels of channeled particles. The energy level is characterized by number i and quasimomentum κ . Thus, the bound energy levels form zone structure. Each zone includes the energy levels with the same number i but with different quasimomentum κ . Due this fact, each zone is characterized by specific width. Eigenvector \mathbf{C}_i corresponds to every energy level ε_i and defines the wave function ψ_i of the given bound state:

$$\psi_i(x) = \frac{1}{\sqrt{a_x}} \sum_n C_n^i \exp(i(\kappa - ng_0)x), \quad n = [-N_{\max}; N_{\max}]. \quad (10)$$

The factor $1/\sqrt{a_x}$ is added to satisfy the normalization condition

$$\int_{-d}^d \psi_i^* \psi_i dx = 1.$$

In Tables 1 and 2 the bound zone structure for $E_{\text{kin}}=80$ MeV (full energy $E=80.5$ MeV) electrons and positrons channeled along (220) planes in Si crystal are presented. The top of potential equals zero for electrons and equals 24.4 eV for positrons. And on the contrary, the deep of potential equals -24.4 eV for electrons and equals zero for positrons. Only sub-barrier zones are presented. Parameters of Si crystal are $a=5.43$ Å as the lattice constant, and $Z_{\text{cr}}=14$ as the atomic number. The location of atoms onto (220) planes is defined by distances $a_x = 1/(2\sqrt{2})a$, $a_y = 1/\sqrt{2}a$, $a_z = a$, $y_{\text{pl}} = 1/(4\sqrt{2})a$, $z_{\text{pl}} = 1/2a$, and (220) plane has the basic $(\rho_y, \rho_z) = (1/(2\sqrt{2})a, 1/2a)$. In our calculations we used $N_{\max}=50$.

Table 1. Sub-barrier zone structure for 80 MeV electrons channeled along (220) Si planes.

Zone number	Down limit of zone, eV	Width of zone, eV	Top limit of zone, eV	Gap between the top limit of this zone and the down limit of the next zone, eV
1	-21.3	$\ll 0.1$	-21.3	5.6
2	-15.7	$\ll 0.1$	-15.7	4.3
3	-11.4	$\ll 0.1$	-11.4	3.1
4	-8.3	$\ll 0.1$	-8.3	2.4
5	-5.9	$\ll 0.1$	-5.9	2.0
6	-3.9	$\ll 0.1$	-3.9	1.6
7	-2.3	$\ll 0.1$	-2.3	1.1
8	-1.1	< 0.1	-1.1	0.8
9	-0.3	0.3	0.0	0.3

Table 2. Sub-barrier zone structure for 80 MeV positrons channeled along (220) Si planes.

Zone number	Down limit of zone, eV	Width of zone, eV	Top limit of zone, eV	Gap between the top limit of this zone and the down limit of the next zone, eV
1	0.6	$\ll 0.1$	0.6	1.3
2	1.9	$\ll 0.1$	1.9	1.4
3	3.3	$\ll 0.1$	3.3	1.4
4	4.7	$\ll 0.1$	4.7	1.4
5	6.1	$\ll 0.1$	6.1	1.4
6	7.5	$\ll 0.1$	7.5	1.4
7	9.0	$\ll 0.1$	9.0	1.5
8	10.6	$\ll 0.1$	10.6	1.6
9	12.2	$\ll 0.1$	12.2	1.6
10	13.8	$\ll 0.1$	13.8	1.7
11	15.5	< 0.1	15.5	1.8
12	17.3	< 0.1	17.3	1.7
13	19.0	0.1	19.1	1.6
14	20.7	0.3	21.0	1.4
15	22.4	0.5	22.9	1.1
16	24.0	0.9	24.9	0.7

3 POPULATIONS OF BOUND STATES

3.1 Initial populations

The initial distribution of channeled particles over transverse energy states is formed when particles penetrate to a crystal. Let us describe the transverse motion of a free particle by the plane wave

$$\psi_0 = \frac{1}{\sqrt{a_x}} \exp\left(\frac{i}{\hbar} p_{\perp} x\right)$$

The probability $P_{0,i}$ of particle capture into the i -th zone defines by the expression:

$$P_{0,i} = \left| \int_{-d}^d \psi_0(x) \psi_i(x) dx \right|^2. \quad (11)$$

It is notable that only elastic captures have been considered, i.e. the transverse momentum of a free particle corresponds to its quasimomentum in the bound state.

In Figs. 2 and 3 the initial populations of bound energy states for $E_{\text{kin}}=80$ MeV electrons and positrons channeled in Si (220) crystal are presented. The projectiles penetrate into the crystal under the glancing angle $\theta=2''$ (about $10 \mu\text{rad}$) to the (220) planes.

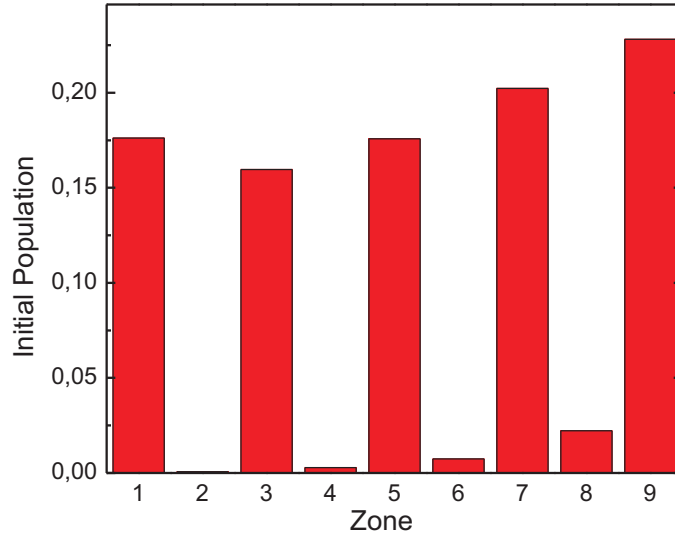


Fig.2. Initial populations of bound states for 80 MeV electrons channeled along (220) Si planes. Angle between momentum of electron and (220) planes is $\theta=2''$. We have chosen non zero incidence angle in order to have the even zones populated.

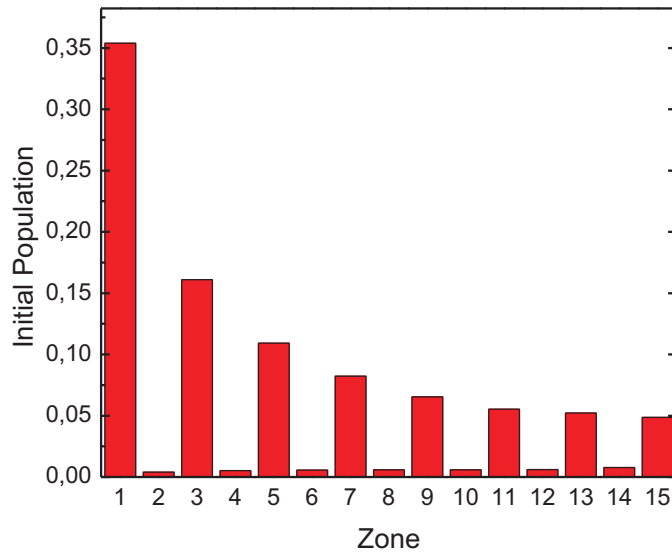


Fig.3. Initial populations of bound energy states for 80 MeV electrons channeled along (220) Si planes. Angle between momentum of positron and (220) planes is $\theta=2''$.

3.2 Dynamics of bound states populations

At particle motion in a crystal, a particle can change its transverse energy under the influence of periodic part of crystal potential. The periodic part of a potential can be considered as perturbation. When kinetic energy of a particle is not large (<120 MeV), the number of sub-barrier energy levels is not very large (about 10-20) and to describe the evolution of bound state populations P_i one can use a system of the kinetic equations in the form [2]:

$$\frac{dP_i}{dt} = \sum_j w_{ij} P_j - \Gamma_i P_i \quad (12)$$

Here w_{ji} is the transition probability from i -th state to j -th state at the unit of time, $\Gamma_i = \sum_j w_{ji}$ is the full probability to leave i -th energy state. Let us calculate the quantities w_{ji} .

The probability of transition from i -th state to j -th state is generally a time-dependent function [4], i.e.

$$W_{ji} = \frac{1}{\hbar^2} \left| \int_0^t V_{ji} \exp(i\omega_{ji}t) dt \right|^2, \quad (13)$$

where t is the time of particle motion in a crystal. The frequency of transition is $\omega_{ji} = (\varepsilon_j - \varepsilon_i)/\hbar$ and V_{ji} is the sum of the matrix elements $\sum_{k_y, k_z \neq 0} \int \psi_i^* U_{k_y, k_z} \psi_j dx \cdot \exp(i(k_y y + k_z z))$. Due to the fact that the amplitudes U_{k_y, k_z} are fast decreasing at n_y and n_z increase, in the first approximation, our consideration can be limited by the term with $(n_y = 1, n_z = 1)$.

Let the angle between longitudinal momentum p_{\parallel} and OY axis be equal to φ . Successfully we can turn OY and OZ axes over the angle φ in order to get OY axis directed along p_{\parallel} (see Fig. 1). In new frame coordinates we can define $y' = v_{\parallel} t$ and $z' = 0$. Using the relations $y = y' \cos \varphi + z' \sin \varphi$ and $z = y' \sin \varphi - z' \cos \varphi$ one can obtain that on the particle's trajectory $\exp[i(k_y y + k_z z)] = \exp[i(k_y \cos \varphi + k_z \sin \varphi) v_{\parallel} t]$. The longitudinal velocity is

$$v_{\parallel} = \sqrt{1 - \frac{1}{\gamma^2}} c \cos \theta.$$

Hence, we can write

$$V_{ji} = \int_{-d}^d \psi_i^* U_{k_y, k_z} \psi_j dx \cdot \exp(i\omega \cdot t). \quad (14)$$

Here $\omega = (k_y \cos \varphi + k_z \sin \varphi) v_{\parallel}$ is the frequency of particle interaction with the crystal field, and, thus, in relations (2) the only element with $(n_y = 1, n_z = 1)$ should be taken into account. After integration in (13), we obtain the following expression

$$\int_0^t V_{ji} \exp(i\omega_{ji}t) dt = -i \frac{G_{ji}}{\omega + \omega_{ji}} (\exp(i(\omega + \omega_{ji}) \cdot t) - 1),$$

where $G_{ji} = \int \psi_i^* U_{k_y, k_z} \psi_j dx$. Hence,

$$W_{ji} = \frac{2|G_{ji}|^2}{\hbar^2 (\omega + \omega_{ji})^2} (1 - \cos(\omega + \omega_{ji})t). \quad (15)$$

Finally, the transition probability at the unit of time is

$$w_{ij} = \frac{dW_{ij}}{dt} = \frac{2|G_{ij}|^2}{\hbar^2 (\omega + \omega_{ij})} |\sin(\omega + \omega_{ij})t| \quad (16)$$

The condition to have the transition probability w_{ij} positive requires considering only absolute value of $\sin(\omega + \omega_{ij})t$.

Calculating the integrals G_{ij} , we have to underline that the wave functions presented by the expansions (10) have chosen only for elastic transitions. Hence,

$$G_{ij} = \sum_{n, m=-N_{\max}}^{N_{\max}} C_n^i C_m^j \int_{-d}^d U_{k_y, k_z}(x) \cos((i-j)g_0 x). \quad (17)$$

Therefore, we obtain that the system (12) contains a lot of time-dependent periodic terms with different frequencies. To solve this system, it should be noted that energies of transition between mostly populated sub-barrier and lowest above-barrier levels are about 10-100 eV. It means that the frequencies ω_{ji} have the values $1.5 \cdot 10^5 \div 1.5 \cdot 10^6 \text{ c}^{-1}$, while characteristic frequencies of crystal field are about 10^8 c^{-1} for the given particle energies and the lattice constant ($\sim 10^{-8} \text{ cm}$). Hence,

$$\omega + \omega_{ji} \approx \omega.$$

Within this approximation the system (12) is reduced to

$$\frac{dP_i}{dt} = \left[\sum_j B_{ij} P_j - B_i P_i \right] |\sin \omega t|, \quad (18)$$

where $B_{ij} = \frac{2|G_{ij}|^2}{\hbar^2 \omega}$, $B_i = \sum_j B_{ij}$.

Obviously, the system (18) is determined by two terms (each term, indeed, represents a system): the first term corresponds to $\sin \omega t \geq 0$, and the second - to $\sin \omega t \leq 0$. The first system (when $\sin \omega t \geq 0$)

$$\frac{dP_i}{dt} = \left[\sum_j B_{ij} P_j - B_i P_i \right] \sin \omega t \quad (19)$$

has a general solution $P_i = A_i \exp(\lambda \cos \omega t)$ at the initial conditions $P_{0,i}$, which are defined by the integrals (11). When general solution is substituted into Eq.(19), one obtains

$$(B_i - \lambda \omega) A_i - \sum_j B_{ij} A_j = 0. \quad (20)$$

The system (20) defines $(2N_{\max}+1)$ eigenvalues λ_j of symmetrical matrix. This matrix has non-diagonal elements, which equal $-B_{ij} / \omega$, and diagonal elements, which equal $(B_i / \omega - 1)$. Each eigenvalue λ_j corresponds to eigenvector $\|A_{ij}\|$; the first index numerates the level's number, and the second index numerates the eigenvalue. Hence, as the eigenvectors $\|A_{ij}\|$ are defined with constant multiplier μ_j accuracy, the general solution should be rewritten in the form

$$P_i = \sum_j \mu_j A_{ij} \exp(\lambda_j \cos \omega t). \quad (21)$$

The initial condition gives:

$$P_{0,i} = \sum_j \mu_j A_{ij} \exp(\lambda_j). \quad (22)$$

Constants μ_j are defined from linear non-homogeneous system (22).

The second system (when $\sin \omega t \leq 0$) is

$$\frac{dP_i}{dt} = \left[-\sum_j B_{ij} P_j + B_i P_i \right] \sin \omega t. \quad (21)$$

It has the same general solution, as the first system: $P_i = A'_i \exp(\lambda'_i \cos \omega t)$, but the initial time moment in this case is defined by $\omega t = \pi$. The initial condition should match the solutions of both systems:

$$P'_{0,i} = \sum_j \mu_j A_{ij} \exp(-\lambda_j). \quad (23)$$

Substituting a general solution into Eq.(19), we obtain

$$(B_i + \lambda' \omega) A'_i - \sum_j B_{ij} A'_j = 0. \quad (24)$$

Comparing Eqs.(20) and (24) one can consider that the system (24) defines $(2N_{\max}+1)$ values λ'_j , where $\lambda'_j = -\lambda_j$, $A'_{ij} = A_{ij}$. Similarly, general solution must be rewritten in the form

$$P_i = \sum_j \mu'_j A_{ij} \exp(-\lambda_j \cos \omega t), \quad (25)$$

where the constants μ'_j are defined from the initial condition (23):

$$P'_{0,i} = \sum_j \mu'_j A_{ij} \exp(\lambda_j) \quad (26)$$

Finally, populations of bound states depend on time as follows:

$$\begin{aligned} P_i &= \sum_j \mu_j A_{ij} \exp(\lambda_i \cos \omega t), & \omega t \geq 0, \\ P_i &= \sum_j \mu'_j A_{ij} \exp(-\lambda_i \cos \omega t), & \omega t \leq 0. \end{aligned} \quad (27)$$

Figs. 4-7 demonstrate the change of populations for some bound states during one period $T = 2\pi / \omega$. Calculations were performed by solving the systems (19) and (21) for $E_{\text{kin}}=80$ MeV electron and positron planar channeling in Si (220) crystal. The angle between momentum of projectiles and (220) planes is $\theta=2^\circ$. The angle between longitudinal momentum and $\langle 110 \rangle$ axis is $\varphi=45^\circ$.

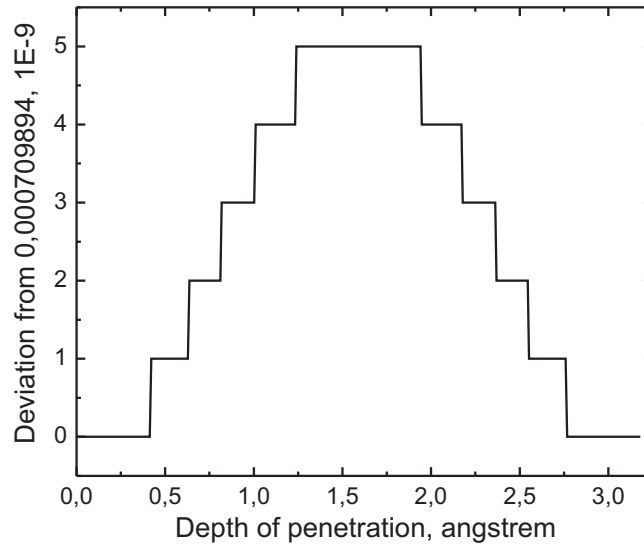


Fig.4. The deviation of population of the 2-nd state from its initial value (0.000709894) as the function of penetration depth. (220) Si planar channeling, kinetic energy of electron - 80 MeV, the angle between momentum of electron and (220) planes - $\theta=2''$, the angle between longitudinal momentum and $\langle 110 \rangle$ axis - $\varphi=45^\circ$.

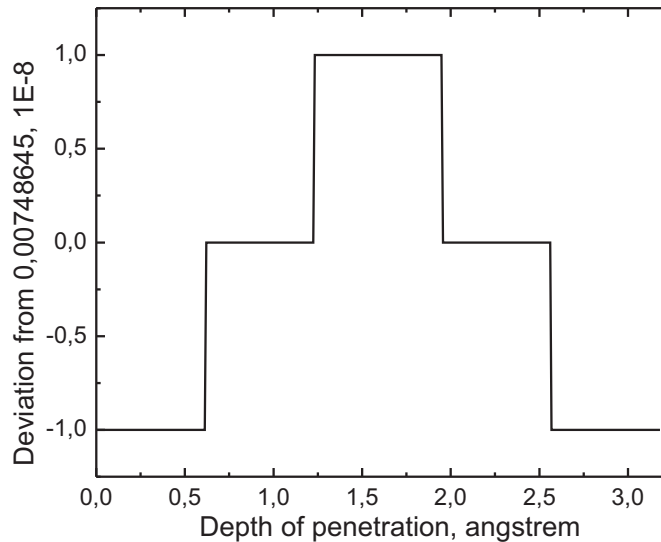


Fig.5. The deviation of population of the 6-th state from its value at 1.5 Å (0.000748645) as the function of penetration depth. (220) Si planar channeling, kinetic energy of electron - 80 MeV, the angle between momentum of electron and (220) planes - $\theta=2''$, the angle between longitudinal momentum and $\langle 110 \rangle$ axis - $\varphi=45^\circ$.

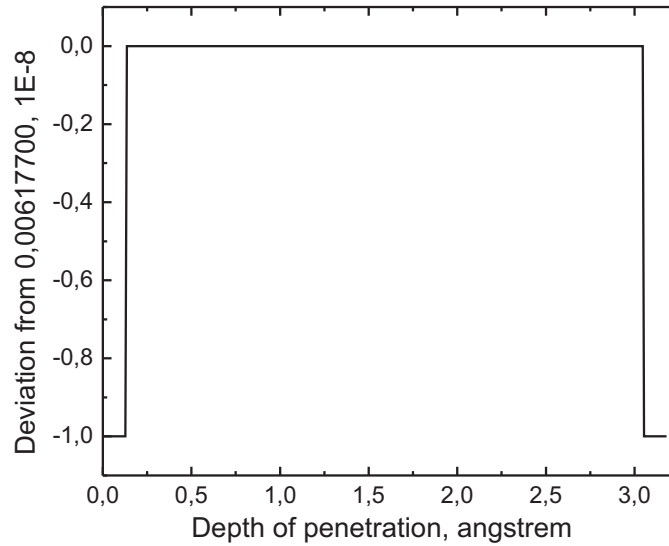


Fig.6. The deviation of population of the 12-th state from its value at 1.5 Å (0.00617700) as the function of penetration depth. (220) Si planar channeling, kinetic energy of positron - 80 MeV, the angle between momentum of positron and (220) planes - $\theta=2''$, the angle between longitudinal momentum and $\langle 110 \rangle$ axis - $\varphi=45^\circ$.

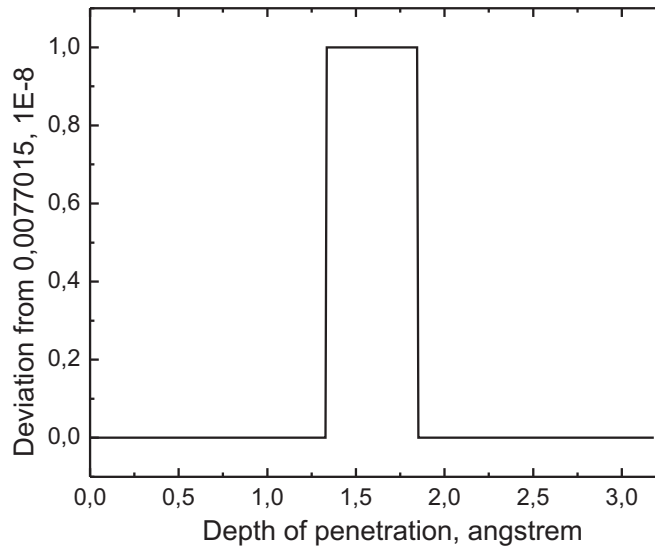


Fig.7. The deviation of population of the 14-th state from its initial value (0.0077015) as the function of penetration depth. (220) Si planar channeling, kinetic energy of positron - 80 MeV, the angle between momentum of positron and (220) planes - $\theta=2''$, the angle between longitudinal momentum and $\langle 110 \rangle$ axis - $\varphi=45^\circ$.

4 DISCUSSION AND CONCLUSION

In this work we analyzed the bound energy spectra and populations for channeled electrons and positrons. We described the algorithms for both constructing bound energies and obtaining the initial populations of the states. We suggested the mathematical model to explore the change of populations during the motion of projectiles through the crystal. The simple approximations used allow analytical solutions of kinetic equations to be obtained.

Presented models have been applied to describe the planar channeling of 80 MeV electrons and positrons along (220) planes in Si crystal.

The bound zone energy structures for these projectiles are defined. For instance, we have shown that electrons have nine sub-barrier zones. The results proved the fact that the width of a zone becomes larger, and the energy gap between neighboring zones decreases, when a zone number increases. For positrons we find sixteen sub-barrier zones. Similar to the case of electrons, the width of zone increases together with the increase of a zone number. But dependence of the gap between neighboring zones has extremum. The gap grows for bottom zones and then gap decreases after 11-th zone. In both cases, for electrons and positrons, the bottom zones are very narrow.

We have evaluated initial populations of sub-barrier energy states for considered projectiles. The initial populations of even states are much less than initial populations of odd states. The dependence of even states populations on zone number is growing for both electrons and positrons, while for odd states populations it is decreasing for positrons and has extremums for electrons. We assumed that the capture of projectiles onto energy state is elastic process. Hence, the particle may be trapped only by the state in a zone where transverse momentum of free particle corresponds to its quasimomentum. In [6] the problem of inelastic capture of projectile was discussed. It was shown, that the account of inelastic capture might change the initial populations of bound energy zones. Nevertheless, inelastic effects are small and might be omitted for simplicity.

We have defined the dynamics of energy states populations; the results of calculations for some sub-barrier states are shown in Figs.4-7. All figures have demonstrated negligible change in populations during the motion of projectiles. Moreover, the change in populations of bottom states is not meaningful, but populations of top states might depend significantly on above-barrier states, which are not included into presented model. Perhaps, to take into account dechanneling processes will change the populations dynamics. Indeed, when particles penetrate into crystal, they populate favorable bound energy levels; transitions between these levels are less probable while the amount of particles is constant (without dechanneling). When projectiles leave the sub-barrier states, other sub-barrier particles may occupy that states (particle exchange between the levels), resulting in such a way in complicated picture for population dynamics. Hence, the model needs improvement and presented results may be considered as previous results only.

REFERENCES

1. J. Lindhard. *Kgl. Dan. Viden. Sels. Mat.-Fys. Medd.*, **34**, 14 (1965).
2. V. A. Basylev, N. K. Zhevago. *Radiation from Fast Particles in a Matter and External Fields*. Moscow, Nauka, 1987 (in Russian).
3. M. A. Kumakhov. *Radiation from Channeled Particles in Crystals*. Moscow, Energoatomizdat, 1986 (in Russian).
4. Donald S. Gemmel. *Reviews of Modern Physics*, v. 44, **1**, p. 129 (1974).
5. L. D. Landau, E. M. Lifshits. *Theoretical Physics. Quantum Electrodynamics*. Moscow, Fizmatlit, 2001 (in Russian).
6. O. V. Bogdanov, K. B. Korotchenko, Yu. L. Pivovarov. *JETP Letters*, v. **85**, 11, p. 555, (2007).